Preparation of Electrode Based on Plasma Modification and Its Electrochemical Application

Kai Wang, Chen Li, and Bingcheng Ji

The carbon nanotubes-manganese oxide (CNTs/MnO$_2$) composite raw material was synthesized through chemical precipitation, and then was modified by the induction-coupled oxygen plasma source to get the improved materials. The influences of the modification effect on the morphology and constitution of the electrode material were investigated with SEM and FT-IR. An oxygen plasma exposure in the coupled plasma source for 20 min at 450 W and 30 Pa leads to a specific capacitance value of 260.2 F/g, i.e., 1.64 times larger than the initial electrode. Its ESR is 0.35 Ω, which decreases by 70.8%. The composite material modified by the oxygen plasma is an excellent electrode material for the supercapacitor that can be used in the electromagnetic launch system and other fields that require high power and energy density.

1. Introduction

Supercapacitor is a kind of electrical device that has high energy and power density, and it has a wide application in the fields ranging from aerospace field to consumer electronic devices. The electrode is the most important part that has a direct influence on the performance of the capacitor (Ref 1-3). Generally, the supercapacitor can be classified into two categories on the basis of the energy storage mechanism, i.e., electric double layer capacitors (EDLCs) and pseudocapacitors (Ref 4, 5). The typical electrode materials of EDLCs are carbon materials with high surface area, which have access to store energy in the double layers on the surface of carbon materials (Ref 6). While in the case of pseudocapacitors, the most used electrode materials are metal oxides and conducting polymers, which can transfer the faradic charges between electrode and electrolyte (Ref 7).

As a newly found carbon material, carbon nanotubes (CNTs) has become one of the most studied materials in the application of engineering fields, such as mechanical engineering, mechanics, and chemical engineering. Because of its unique physical, chemical, electrical, and mechanical properties, this new material has shown promising prospects for several advanced applications, including supercapacitors, fuel cells, chemical detectors, and solar cells (Ref 8). Recently, the application of CNTs in supercapacitors has been measured by some researchers. For instance, Stoller et al. (Ref 9) and Wang

et al. (Ref 10) reported that the supercapacitor devices based on CNTs materials exhibited good electrochemical performance. However, the actual capacitive behavior of pure CNTs is much lower than the anticipated value due to the fact that it usually suffers from serious agglomeration during preparation. To boost the electrochemical performance of CNTs-based supercapacitor remains a great challenge. On the other hand, the attempt of using the combination effect of the double layer capacitor and pseudocapacitor has been made to boost the electrochemical performance of the composite electrode. It has been found that carbon materials combined with pseudocapacitive electrode materials, such as MnO$_2$, Ni(OH)$_2$, RuO$_2$, polyaniline (PANI), and polypyrrole (PPy), can improve the capacitance of carbon (Ref 11-13).

As a new kind of treatment method, the surface modification technique by oxygen plasma has been widely used in the modification of electronic materials and mechanical products. Daffos et al. (Ref 14) have synthesized the spark plasma sintered carbon electrodes for capacitors which have a maximum specific capacitance of 110 F/g. Due to its strong oxidative activity and convenient preparation, the oxygen plasma has been recognized as a good candidate in the field of surface modification.

In this paper, we propose the synthesis and oxygen plasma modification method of the CNTs/MnO$_2$ composite for supercapacitor applications, and some experiments were carried out to investigate the relation between the modification treatment and the electrochemical properties of the composite material.

2. Experimental

2.1 Preparation of the CNTs/MnO$_2$ Composite Electrode Materials

The nanocomposites were synthesized by chemical coprecipitation method. First, 0.75 g KMnO$_4$ and 1.837 g Mn(AC)$_2$ were mixed in 50 mL deionized water, which was in order to

Kai Wang, School of Automation Engineering, Qingdao University, Qingdao 266071 Shandong, China; Chen Li, School of Electrical Engineering and Automation, Tianjin Polytechnic University, Tianjin 300384, China; and Bingcheng Ji, School of Electrical Engineering, Dalian University of Technology, Dalian 116023 Liaoning, China. Contact e-mail: wang_kai1985@163.com.
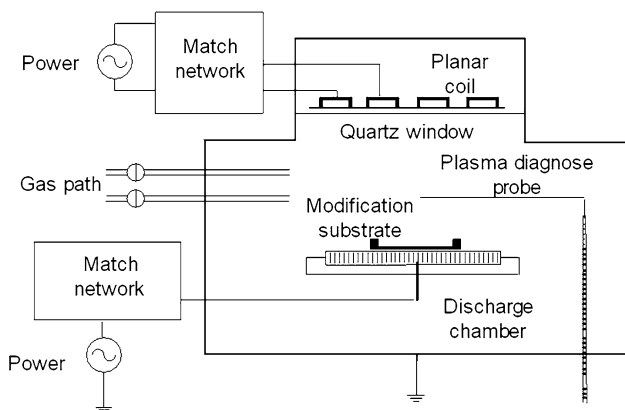
Fig. 1 The picture and schematic diagram of coupled plasma resource

get the solution with the concentration of 0.1 M. Then 0.75 g CNT (MWNT 2040, shenzhen nanoport) was added into the KMnO$_4$ solution and magnetic stirred for 1 h to make solutions dispersed evenly. Afterward, Mn(AC)$_2$ was added into the CNT and KMnO$_4$ mixed solution. Then the obtained products were filtrated and washed several times with distilled water, and then dried at 80 °C in vacuum oven for 12 h. The resultant products were well ground into powders and collected for further use. For convenience, this electrode material before the oxygen plasma modification treatment was denoted as sample A.

2.2 Oxygen Plasma Modification of the Electrode Material

Figure 1 shows the picture and schematic diagram of coupled plasma source. On the top, there is a quartz window with a diameter of 20 cm and a thickness of 1.2 cm, which is used to transmit the radio frequency power into the plasma. On the quartz disk, there is a two-turn planar coupling coil with an outer diameter of 8 cm and an inner diameter of 6 cm. The radio frequency power is supplied at 13.56 MHz and connected to a coil via a match network. Its output power is in the range of 0-1500 W. The products collected from the above procedures were positioned in the center of the discharge chamber, and then the chamber was pumped to the pressure less than 4×10^{-3} Pa before modification. Afterward, the oxygen gas (purity > 99.995%) regulated by a mass flow controller was fed into the discharge chamber through a gas distributor at the speed of 7 sccm (standard cubic centimeters per minute) until the gas pressure was adjusted to 30 Pa. Then the plasma source began to discharge (at a moderate power of 450 W). The modification treatment is conducted for 10, 20, and 30 min, respectively. Meanwhile, the products were dewatered in the chamber. Finally, the materials were taken out and used for characterization. Each time three-electrode samples were prepared following the same procedures mentioned above, and denoted as sample B, C, D, respectively.

2.3 Characterization and Analysis on the Sample Materials

The morphological observation of the samples was carried out using a Hitachi S-4800 field emission SEM. Analysis on the samples' constitution was performed on a IR Prestige-21 FT-IR spectrometer (KBr pelleting) over the wave number range of 400-4000 cm^{-1}. The electrochemical performances of the samples were obtained by the CHI608A electrochemical

working station (Chenhua Instrument, Shanghai, Inc). Galvanostatic charges-discharge experiments were conducted within the capacitors of the symmetric electrodes over the potential range of 0-1.2 V. All the measurements were carried out in 1 M Na$_2$SO$_4$ solution at 25 °C.

3. Results and Discussion

### 3.1 Morphology and FT-IR Spectra of the Electrode Materials

The SEM images of the composite materials are shown in Fig. 2. All the samples show a distinct reticular structure. After exposing the substrates to oxygen plasma, the samples B and C seem to have a uniform distribution with few irregularly aggregations, but the sample D that was modified for 30 min seem to have a little aggregation. In all, there are no clear differences between the four pictures. The FT-IR spectra of the samples are shown in Fig. 3. In the spectra of the four samples, the band at 3440 cm^{-1} should be ascribed to the O-H stretching vibration; the band at 1630 and 1110 cm^{-1} should be ascribed to the O-H and the Mn atom bending vibration. The wide bands at 560 and 530 cm^{-1} are usually ascribed to the Mn-O bending vibration. The FT-IR spectra of the samples appear the same except that the O-H absorption peaks of the samples B, C, and D are strongly enhanced compared with sample A, which reveals that the hydroxyl functional groups were introduced after the oxygen plasma modification treatment.

3.2 Electrochemical Measurement of the Electrode Materials

3.2.1 Electrochemical Impedance Measurements. Figure 4 shows the electrochemical impedance spectra of the samples. The electrochemical impedance spectroscopy (EIS) was tested with a three-electrode system in which each of the electrode samples was used as the working electrode, respectively, a saturation calomel (SCE) as the reference electrode, and a Pt wire as the counter electrode. The measurement was carried out within the frequency range of 10^{-2} to 10^5 Hz. The offset voltage was set to 0 V (vs. SCE). It can be seen that each Nyquist plot consists of a high-frequency arc and a low-frequency spike. The high-frequency arc corresponds to the charge transfer resistance at the electrode/electrolyte interface, and the low-frequency spike corresponds to the Warburg impedance of Na$^+$ diffusion into the CNTs/MnO$_2$ composite material. As can be seen, there is a difference between every two high-frequency arcs of the four electrodes, indicating the charge transfer resistance of the sample decreases with increasing time of the oxygen plasma modification treatment, but the overall impedance of sample D is larger than that of sample C. We suppose that this is due to the fact that the electrons and ions ionized from the discharge of the oxygen plasma have a intense etch on the surface of the composite materials after the modification, at the same time the well-distributed electrons and ions show a perfect guidance to the distribution of MnO$_2$ particles. It means that the ESR is low and helpful for the electrochemical performance. In addition, after this procedure the skeleton of CNTs can be evenly surrounded by the MnO$_2$ nanoparticles. A large amount of hydroxyl functional groups are introduced on the surface of the composite materials. Hence, both the conductivity and the
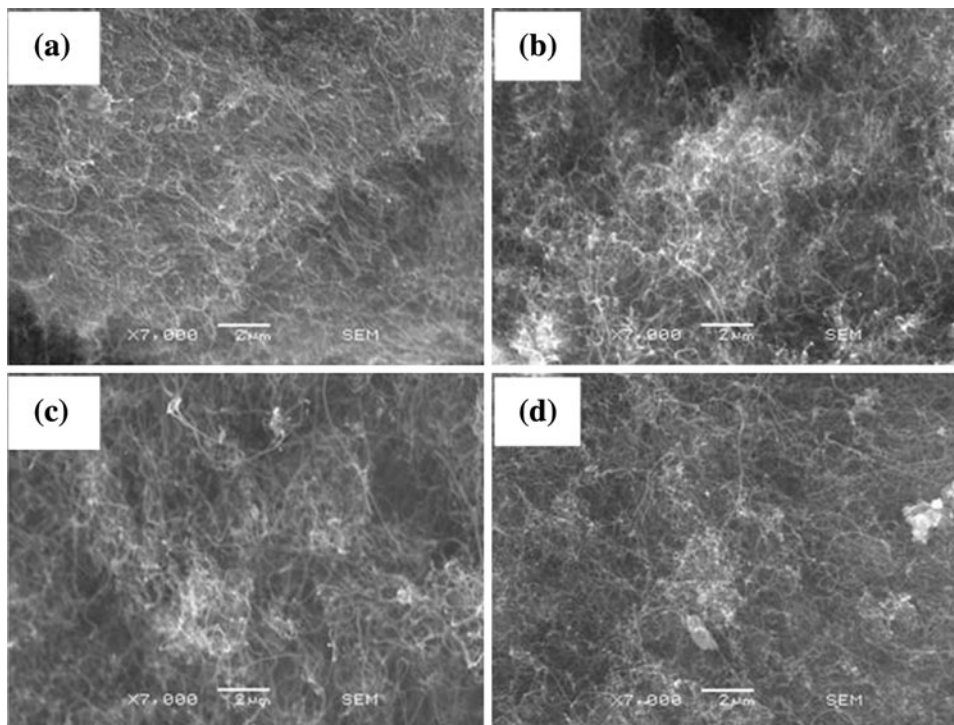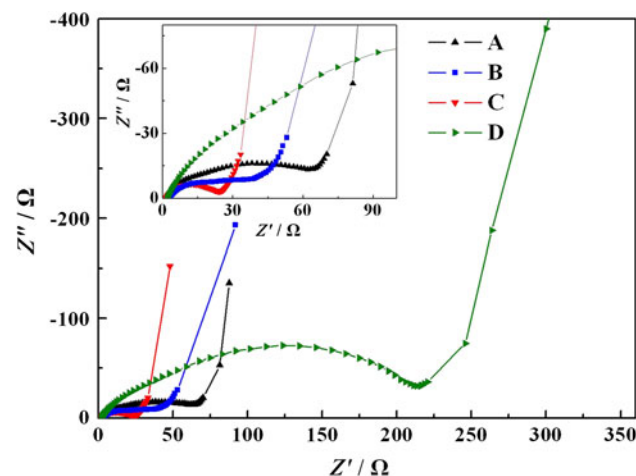
Fig. 2 The SEM images of each materials before and after the oxygen plasma treatment. (a) No treatment, (b) 10 min, (c) 20 min, (d) 30 min
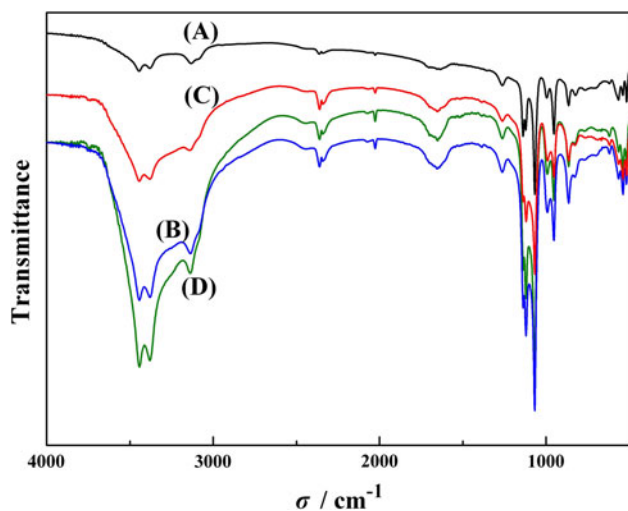
Fig. 3 The FT-IR spectra of the samples before and after the oxygen plasma treatment. (a) No treatment, (b) 10 min, (c) 20 min, (d) 30 min

Fig. 4 Nyquist plots of the electrode samples before and after the oxygen plasma treatment. (a) No treatment, (b) 10 min, (c) 20 min, (d) 30 min

capacitive performance of the $CNTs/MnO_2$ composites are improved through the modification. However, the Warburg impedance of sample D is larger compared with the other samples, which indicates a large diffusion resistance that exists inside the porous material.

On the basis of the electrochemical impedance spectra, the equivalent series resistance (ESR) of sample A and C are 1.2 and 0.35 Ω, respectively. This result indicates the ESR of sample C decreased by 70.8% compared with that of sample A. It may be due to the fact that during the modification, the conductivity of the composite materials is improved (Ref 15). Its surface free energy is also changed during the treatment; as a result the wettability of the composites is improved. From this point of view, the Na^+ and SO_4^{2-} in the electrolyte can penetrate deeply inside the micropores, and the charge transfer resistance is decreased, so the ESR of the $CNTs/MnO_2$ composite materials is decreased due to the oxygen plasma modification treatment.

3.2.2 Charge-Discharge Test. With nickel foam as the current collector, non-woven fabrics as the membrane, and 1 M Na_2SO_4 aqueous solution as the electrolyte, we use each of sample materials to assemble supercapacitors that have symmetric electrodes. The supercapacitors were charged and discharged within the operating voltage range of 0-1.2 V at a current density of 1 A/g (current divided by the overall weight
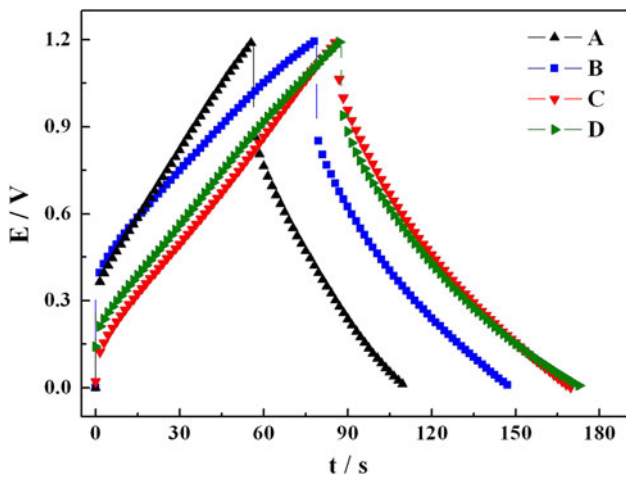
Fig. 5 The charge-discharge plots of supercapacitors assembled by the materials before and after the oxygen plasma treatment. (a) No treatment, (b) 10 min, (c) 20 min, (d) 30 min
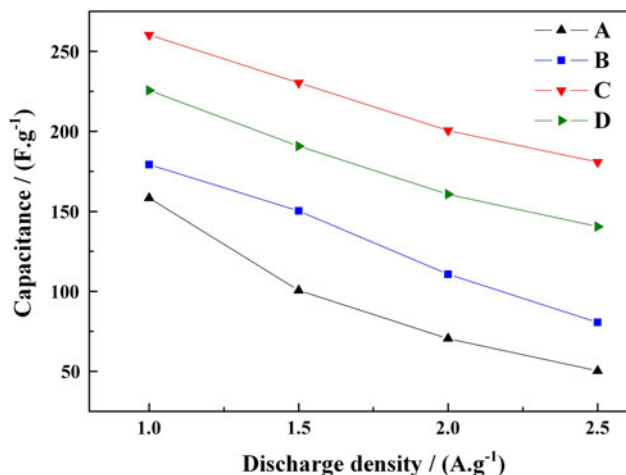
Fig. 6 Capacitance curves of supercapacitors under different current densities. (a) No treatment, (b) 10 min, (c) 20 min, (d) 30 min

of the positive and negative active materials). In Fig. 5, the charge-discharge profiles show a shape of isosceles triangle approximately, suggesting a good electrochemical reversibility. And the instantaneous voltage drop at the beginning of discharge process for each sample decreases successively under the same current density, which means the ESR of each capacitor decreases with increasing the time of the modification.

The specific capacitance of each sample calculated from Fig. 5 is 158.4, 179.3, 260.2, and 225.6 F/g, respectively, which indicates that the specific capacitance of sample C is approximately 1.64 times of sample A. These results may be attributed to the fact that the hydroxyl functional groups are introduced on the surface of CNTs/MnO$_2$ composite materials during the oxygen plasma modification, which brings the pseudocapacitance to the supercapacitor. Nevertheless, the reason for the smaller specific capacitance of sample D compared with sample C is that the aggregation is enhanced after a long time of modification treatment, which not only prevents the electrode material to have a good contact with the electrolyte but also results in a decrease of the specific capacitance of sample D finally.

The capacitance curves of the supercapacitors made of each electrode samples are shown in Fig. 6. The specific capacitance of sample C is the largest among all the samples and it has a good retention of the capacitance from 260.2 to 180.6 F/g when the current density was increased from 1 to 2.5 A/g, which indicates that the sample C has a good rate capability and can be used in the high power fields.

4. Conclusions

CNTs/MnO$_2$ composite materials were synthesized through chemical coprecipitation method, and then they were modified by the oxygen plasma. The electrochemical measurement reveals that the CNTs/MnO$_2$ composite material modified by oxygen plasma for 20 min has perfect electrochemical performance and its specific capacitance is 260.2 F/g, which is 1.64 times of the electrode material without modification. Meanwhile, its ESR is 0.35 Ω, which decreases by 70.8%. The SEM and FT-IR indicated that the hydroxyl functional groups were gradually introduced on the surface of CNTs/MnO$_2$ composite materials, and the morphology of the composites appeared more homogeneous after the modification. The CNTs/MnO$_2$ composites based on the oxygen plasma modification treatment show promising prospects in the supercapacitors that require to be charged and discharged at the high power, and at the same time it reveals that the oxygen plasma modification is an effective and economical treatment method.

References

1. P. Simon and Y. Gogotsi, Materials for Electrochemical Capacitors, *Nat. Mater.*, 2008, **7**(11), p 845–854
2. W. Xing, C.C. Huang, and S.P. Zhuo, Hierarchical Porous Carbons with High Performance for Supercapacitor Electrodes, *Carbon*, 2009, **47**(7), p 1715–1722
3. K. Wang and L. Zhang, Synthesis of Ordered Mesoporous Carbon and Its Electrochemical Performances, *Int. J. Electrochem. Sci.*, 2013, **8**(2), p 2892–2897
4. R. Kötz and M. Carlen, Principles and Applications of Electrochemical Capacitors, *Electrochim. Acta*, 2000, **45**(15-16), p 2483–2498
5. L. Yang, H. Liu, and Y. Chen, Formation Process of FeCl$_3$-NiCl$_2$-Graphite Intercalation Compounds, *J. Mater. Eng. Perform.*, 2012, **21**(3), p 339–344
6. Y.S. Hu, Y.G. Guo, and W. Sigle, Electrochemical Lithiation Synthesis of Nanoporous Materials with Superior Catalytic and Capacitive Activity, *Nat. Mater.*, 2006, **5**(9), p 713–717
7. X. Xia, H. Liu, and L. Shi, Tobacco Stem-Based Activated Carbons for High Performance Supercapacitors, *J. Mater. Eng. Perform.*, 2012, **21**, p 1956–1961
8. C. Xu, B. Li, and H. Du, Supercapacitive Studies on Amorphous MnO$_2$ in Mild Solutions, *J. Power Sources*, 2008, **184**(2), p 691–694
9. M.D. Stoller, S. Park, and Y. Zhu, Graphene-Based Ultracapacitors, *Nano Lett.*, 2008, **8**(10), p 3498–3502
10. Y. Wang, Z. Shi, and Y. Huang, Supercapacitor Devices Based on Graphene Materials, *J. Phys. Chem. C*, 2009, **113**(30), p 13103–13107

11. G. Wang, L. Zhang, and J. Zhang, A Review of Electrode Materials for Electrochemical Supercapacitors, *Chem. Soc. Rev.*, 2011, **41**(2), p 797–828

12. K. Wang and L. Zhang, The Preparation of Nickel Hydroxide Based on Infinite Dilute Method and its Electrochemical Performance, *Electrochemistry*, 2013, **81**(4), p 259–261

13. K. Wang, L. Zhang, and B. Ji, The Thermal Analysis on the Stackable Supercapacitor, *Energy*, 2013, **59**, p 440–444

14. B. Daffos, G. Chevallier, and C. Estournès, Spark Plasma Sintered Carbon Electrodes for Electrical Double Layer Capacitor Applications, *J. Power Sources*, 2011, **196**(3), p 1620–1625

15. S.-B. Ma, K.-W. Nam, and W.-S. Yoon, Electrochemical Properties of Manganese Oxide Coated onto Carbon Nanotubes for Energy-Storage Applications, *J. Power Sources*, 2008, **178**(1), p 483–489